A computerized tomography study of the morphological interrelationship between the temporal bones and the craniofacial complex

Data · September 2015

CITATIONS
2

READS
837

3 authors, including:

Helder Nunes Costa
Cooperativa de Ensino Superior Egas Moniz
19 PUBLICATIONS **37** CITATIONS

SEE PROFILE

Journal of Anatomy

J. Anat. (2012) **220**, pp544–554 doi: 10.1111/j.1469-7580.2012.01499.x

A computerized tomography study of the morphological interrelationship between the temporal bones and the craniofacial complex

Helder Nunes Costa,[1,2] Rudolf Slavicek[3] and Sadao Sato[1]

[1]*Division of Orthodontics, Department of Craniofacial Growth and Development Dentistry, Kanagawa Dental College, Yokosuka, Japan*
[2]*Instituto Superior de Ciências da Saúde Egas Moniz, CiiEM, Monte de Caparica, Portugal*
[3]*Department of Interdisciplinary Dentistry and Technology, Danube-University, Krems, Austria*

Abstract

The hypothesis that the temporal bones are at the center of the dynamics of the craniofacial complex, directly influencing facial morphology, has been put forward long ago. This study examines the role of the spatial positioning of temporal bones (frontal and sagittal inclination) in terms of influencing overall facial morphology. Several 3D linear, angular and orthogonal measurements obtained through computerized analysis of virtual models of 163 modern human skulls reconstructed from cone-beam computed tomography images were analyzed and correlated. Additionally, the sample was divided into two subgroups based on the median value of temporal bone sagittal inclination [anterior rotation group (n = 82); posterior rotation group (n = 81)], and differences between groups evaluated. Correlation coefficients showed that sagittal inclination of the temporal bone was significantly ($P < 0.01$) related to midline flexion, transversal width and anterior–posterior length of the basicranium, to the anterior–posterior positioning of the mandible and maxilla, and posterior midfacial height. Frontal inclination of the temporal bone was significantly related ($P < 0.01$) to basicranium anterior–posterior and transversal dimensions, and to posterior midfacial height. In comparison with the posterior rotation group, the anterior rotation group presented a less flexed and anterior–posteriorly longer cranial base, a narrower skull, porion and the articular eminence located more superiorly and posteriorly, a shorter posterior midfacial height, the palatal plane rotated clockwise, a more retrognathic maxilla and mandible, and the upper posterior occlusal plane more inclined and posteriorly located. The results suggest that differences in craniofacial morphology are highly integrated with differences in the positional relationship of the temporal bones. The sagittal inclination of the temporal bone seems to have a greater impact on the 3D morphology of the craniofacial complex than frontal inclination.

Key words: 3D cephalometry; cone-beam computed tomography; cranial base; craniofacial morphology; lateral basicranium; temporal bone.

Introduction

Many researchers support the idea that the basicranium plays an important role in influencing overall skull growth (Young, 1916; Weidenreich, 1941; Björk, 1955; Enlow & McNamara, 1973; Lavelle, 1979; Enlow et al. 1982; Anderson & Popovich, 1983; Ellis & McNamara, 1984; Enlow & Bhatt, 1984; Kerr & Adams, 1988; Bacon et al. 1992; Ross & Ravosa, 1993; Ross & Henneberg, 1995; Enlow & Hans, 1996; Baccetti et al. 1997; Singh et al. 1997; Spoor, 1997; Lieberman & McCarthy, 1999; Lieberman et al. 2000, 2008; Bastir et al. 2004; Ross et al. 2004; Bastir & Rosas, 2005, 2006). This is so mainly for three reasons (Lieberman et al. 2008). First, basicranial growth (endochondral ossification) may be under more intrinsic control than facial and neurocranial growth (intramembranous ossification) (Scott, 1958). Second, because the basicranium completes its development earlier in ontogeny than the neurocranium and face, it may limit subsequent characteristics of neurocranial and facial growth (Bastir et al. 2006). Third, the basicranium comprises the central axis of the skull, being closely related to the brain and neurocranium growing above, and the face growing

Correspondence
Helder Nunes Costa, Division of Orthodontics, Department of Craniofacial Growth and Development Dentistry, Kanagawa Dental College, 82 Inaoka-cho, Yokosuka-chi, Kanagawa, 238-8580 Japan.
E: hnc@netcabo.pt

Accepted for publication *28 February 2012*
Article published online *28 March 2012*

below, and it provides all the necessary foramina through which the brain connects to the face and the body. Both midline and non-midline structures of the basicranium seem to be important and may influence the morphology of the face and have relevance in its normal range and possibly even in its pathological range. However, there is still a lack of a comprehensive, predictive theory about how much, to what extent, and how the different parts of the cranial base influence the structure of the skull as a whole.

Bastir et al. (2006) have suggested that the real interface between the neurocranium and the face may be located at the lateral skull base and not at the midline. The bending of the midline of the skull base seems to be set relatively early in ontogenesis, while the face completes its development much later. This may be one reason for the weak correlations between facial pattern and the angle of the skull base (Lieberman et al. 2000). However, the lateral basicranium continues its maturation until late in puberty, and thus shares a common ontogenetic route with the face (Buschang et al. 1983; Bastir et al. 2006), requiring coordinated development processes that may result in greater co-morphological variation. Thus, variations in the lateral basicranium morphology likely have consequences for the spatial arrangement of facial structures (Bastir et al. 2004).

Sato (2002) has hypothesized that the temporal bones are at the center of the dynamics of the craniofacial complex. Located in the lateral-most aspect of the skull, they interact during growth and development with the temporal lobes, the midface and the mandible (Sato, 2002; Bastir et al. 2004, 2008). The temporal bones connect directly with the mandibular condyles forming a very dynamic functional unit highly influenced by the occlusion. They also connect with the parietal bone through a 'sliding joint', the second most dynamic suture of the craniofacial complex. They have the potential to influence cranial base spheno-occipital balance through their articulation with the sphenoid and occipital bones near the midline. The zygomatic process extends forward from the squama and articulates with the malar bone in the face. Besides participating in forming the neurocranium, they also house the apparatus of hearing and balance, and are one surface of attachment for neck and throat muscles. Additionally, two of the primary muscles of mastication, temporalis and masseter muscles, have their insertions on the temporal bone, exerting powerful forces on contraction, directly influencing their positional dynamics. Its complex array of morphology is therefore relevant to several functional systems and dense with potential phylogenetic information (Harvati, 2003; Smith et al. 2007; Lieberman et al. 2008).

This study focuses on the role of the lateral basicranium, particularly the spatial positioning of the temporal bones (frontal and sagittal inclination), in terms of influencing overall facial morphology. According to Sato's hypotheses (Sato, 2002) regarding the dynamic functional anatomy of the craniofacial complex (Fig. 1), an increased flexion of the skull base promotes a clockwise rotation of the sphenoid bone. This rotation transfers a downward vertical force, through the vomer bone to the maxillary complex, leading to the vertical elongation of this complex. This vertical elongation limits the antero-posterior growth of the maxillary complex, causing posterior discrepancy (crowding), which in turn motivates an excessive eruption of the maxillary molars, creating an excessively horizontal maxillary (upper) posterior occlusal plane. The mandible then has to adapt to this occlusal plane in order to keep occlusal function, and does so by anterior rotation. This anterior rotational adap-

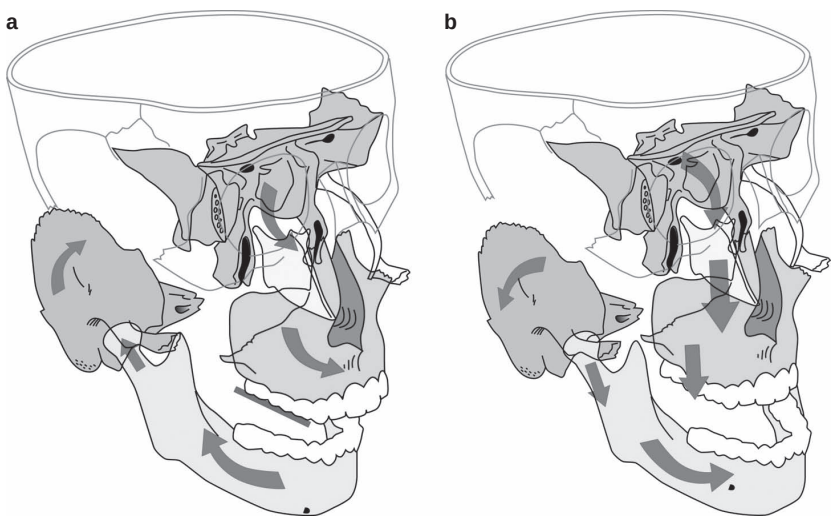

Fig. 1 Model of craniofacial dynamics. Internal (a) or external (b) rotation of the temporal bones influences extension or flexion of the spheno-occipital synchondrosis. The altered spatial positioning of the sphenoid bone then influences, through the vomer bone, the maxillary complex. The vertical dimension of this complex together with the inclination of the posterior upper occlusal plane influence anterior–posterior positioning of the mandible, which in turn further influences the temporal bones and again stimulates the cycle. See text for further details on the model.

tation of the mandible promoted by the neuromuscular system has two effects. On one hand, it leads to a decompression of the condyles, which then grow secondary, and at the same time it diminishes the compression exerted on the mandibular fossa of the temporal bone, which in combination with the traction effect exerted by the chewing muscles (masseter and temporal) suffers external rotation. The skull thus assumes a greater transverse dimension. This external rotation of the temporal bone, through its direct connection with the sphenoid and occipital bones near the midline, influences flexion of the spheno-occipital synchondrosis. This bending of the midline bones determines a smaller anterior–posterior skull base, while influencing further clockwise rotation of the sphenoid bone, which again drives this cycle. An increased extension of the cranial base would have the reverse effect on the craniofacial complex: a steeper upper posterior occlusal plane, lower vertical dimension, a more retrognathic mandible and internal rotation of the temporal bones, accompanied by an anterior–posteriorly longer and transversally narrower skull base.

The complex detailed internal 3D morphology of the temporal bone has proven difficult to study on conventional 2D radiographs. The introduction of cone-beam computed tomography (CBCT) has allowed for 3D volumetric reconstruction of the entire craniofacial complex with great precision (Lagravère et al. 2008; Periago et al. 2008; Brown et al. 2009) and reproducibility (Muramatsu et al. 2008), dramatically improving our ability to understand the 3D nature of craniofacial structures (Vannier et al. 1984).

Materials and methods

Three-dimensional virtual models of human skulls reconstructed from CBCT images were used to test the hypothesis that spatial positioning of the temporal bones influences overall facial morphology. The sample consisted of 163 European adult dry skull specimens from the Weisbach Collection of the Natural History Museum of Vienna. Most were soldiers of the Austro-Hungarian Imperial Army who died or were killed circa 1870. The inclusion criteria for the skulls examined were: no cranial deformity; complete skull bone structure; and the presence of a clinically acceptable and reproducible permanent occlusion with stable mandibular position.

A custom plastic head holder was constructed to support the skulls during imaging and fitted with a laser marker, according to the manufacturer's instructions. To ensure a detailed 3D representation of the occlusal morphology of the maxillary dentition the skulls were also scanned without the mandible present. CBCT scans were acquired with a Galileo Compact system (®Sirona Dental Systems GmbH, Germany). The scanning time was $\sim$ 14 s, and 200 single exposures were performed for each skull with a 3D resolution (isotropic voxel size) of 0.3 mm and 15 cm diameter $\times$ 15 cm height field of view using Sidexis XG acquisition software (®Sirona Dental System GmbH). Exposure parameters were controlled by automatic exposure control. CBCT data were then exported from the Sidexis XG software in Dicom multi-file format and imported into Maxilim® software (version 2.3.0.3, Medicim®, Belgium). Three-dimensional surface models were obtained using the software's automatic thresholding for hard tissue type models and reevaluated by a single calibrated operator on the basis of the following criteria: quality of the 3D morphology; and the presence of relevant skeletal structures.

A 3D craniometric analysis was designed with 26 different landmarks (Table 1). A CT-based reference plane was set up as defined and validated by Swennen (Swennen et al. 2006): the virtual models are first positioned in a standardized way from the lateral and frontal directions; the software then produces virtual lateral and frontal cephalograms after which the reference planes that define an anatomically based frame are set up (Table 2).

Landmark 3D coordinates, 17 angular and 14 linear measurements were designed, obtained and exported with the original skull identification number to Excel files (Microsoft® Excel® 2007, Microsoft). Landmarks were located and marked on the 3D surface-rendered volumetric image of the skull using a laser mouse on a 58.4 cm (23 inch) flat LED screen (Samsung, South Korea). All craniometric measurements were developed by a single observer (HNC).

Landmarks were chosen in order to allow characterization and measurement of the spatial positioning of the temporal bones, midline basicranium, maxilla, upper dentition and jaw sagittal relationship. Landmarks and measurements used in this study are defined in Tables 1 and 3, and illustrated in Figs 2–6.

On both left and right temporal bones four different landmarks were identified: porion (Po), temporal point (T), sphenotemporal point (ST) and articular eminence (AE). Landmarks Po, T and ST were used to calculate the sagittal and frontal inclinations of the temporal bones (Figs 3 and 4). Mean values of the left and right side temporal bone sagittal and frontal inclinations were calculated and used for the statistical analyses. Landmark AE was used to locate the articular eminence of the mandibular fossa. Landmarks basion (Ba), sella (S) and nasion (N) were used for the midline basicranium. Midline basicranium linear measurements were calculated both as length and depth. Length measures the 3D linear distance between two landmarks, whereas depth measures the same distance but without considering the vertical distance between landmarks (parallel to the HRP; Fig. 5). Landmarks anterior nasal spine (ANS), posterior nasal spine (PNS) and A-point (A) were used for the maxilla. On the mandible, B-point was located for calculation of mandibular position ($\angle$SNB) and jaw sagittal relationship ($\angle$ANB).

On the maxillary dentition occlusal landmarks were identified for central incisors, second premolars and second molars. The connecting line between the mandibular stamp cusps of molars and premolars, canine tips and incisal edges represents the line of active centric (Slavicek, 1984; Celar et al. 1994; Costa et al. 2011), i.e. the main line of function. The lower arch is an active arch, and its contact with the maxillary teeth creates the corresponding line of passive centric (marginal ridges of the upper incisors, mesial marginal ridge of the canine and premolars, as well as marginal ridges and grooves of the molars). In an ideal occlusion both the active and passive centric lines coincide. The guiding surfaces of the maxillary teeth, in an angle class I relation, are located on the mesial and distal marginal ridges of both incisors and the mesial marginal ridges of the canines, premolars and first molars. The starting point and ending point of this guidance are called function points. Function points F1 are defined by occlusal contacts in maximum intercuspation. They are the starting points for eccentric movement and therefore belong to the passive centric line. In this study, function points F1 were defined as described in Table 1. To evaluate

Table 1 Definition of anatomic 3D landmarks used in this study.

Landmark	Abbreviation	Definition on CT image
Nasion	N	Midpoint of the frontonasal suture
Sella	S	Center of the hypophyseal fossa (sella turcica)
Basion	Ba	Most anterior point of the foramen magnum
Porion	Por, Pol	Most superior point of the right (Por) and left (Pol) outer acoustic meatus
Mean porion	Po.mean	3D point, computer calculated in the middle of landmarks Por and Pol
Articular eminence	AEr; AEl	Point of inflection from the concavity of the floor of the right (AEr) and left (AEl) mandibular fossa to the flat part of the articular eminence in the middle from a lateromedial aspect
Mean articular eminence	AE.mean	3D point, computer calculated in the middle of landmarks AEr and AEl
Right spheno-temporal point	STr	Point on the external surface of the right spheno-temporal suture coinciding with the vertical reference plane
Left spheno-temporal point	STl	Point on the external surface of the left spheno-temporal suture coinciding with the vertical reference plane
Right temporal point	Tr	Point on the outer surface of the right temporal squama where the vertical reference plane (VRP) meets the horizontal reference plane (HRP)
Left temporal point	Tl	Point on the outer surface of the left temporal squama where the vertical reference plane (VRP) meets the horizontal reference plane (HRP)
Anterior nasal spine	ANS	The most anterior midpoint of the anterior nasal spine of the maxilla
Posterior nasal spine	PNS	The most posterior midpoint of the posterior nasal spine of the palatine bone
A-point	A	Point of maximum concavity in the midline of the alveolar process of the maxilla
B-point	B	Point of maximum concavity in the midline of the alveolar process of the mandible
Center incisor functional point F1	11F1; 21F1	The cervically located point of inflection from the convexity of the tuberculum to the concavity of the palatal surface on the mesial marginal ridge of tooth 11 and 21
Mean center incisor functional point F1	11/21F1	3D point, computer calculated in the middle of landmarks 11F1 and 21F1
2nd premolar functional point F1	15F1; 25F1	Point where the central fissure crosses the mesial marginal ridge on tooth 15 and 25
Mean 2nd premolar functional point F1	15/25F1	3D point, computer calculated in the middle of landmarks 15F1 and 25F1
2nd molar functional point F1	17F1; 27F1	Point where the central fissure crosses the mesial marginal ridge on tooth 17 and 27
Mean 2nd molar functional point F1	17/27F1	3D point, computer calculated in the middle of landmarks 17F1 and 27F1

Table 2 Definition of relevant 3D planes used in the analysis.

Plane	Abbreviation	Definition
Horizontal 3D reference plane (*x*-axis)	HRP	Plane 6° below the anterior cranial base plane (S-N), with the origin in landmark Sella
Median 3D reference plane (*y*-axis)	MRP	Plane containing landmarks Sella and Nasion, perpendicular to the horizontal 3D craniometric reference plane (HRP)
Vertical 3D reference plane (*z*-axis)	VRP	Plane with the origin in landmark Sella and perpendicular to the horizontal and median 3D craniometric reference planes
Frankfort horizontal plane	FH	Plane that passes both orbital landmarks and the computerized 3D mean point between right and left porion landmarks
Palatal plane	PP	Plane that passes through ANS-PNS line, perpendicular to the median 3D craniometric reference plane (MRP)

maxillary (upper) occlusal plane, the mean inclination of left and right passive centric lines of occlusion was determined. Three additional occlusal landmarks were computer generated as the middle points between left and right F1 landmarks of central incisors (teeth 11 and 21), second premolars (teeth 15 and 25) and second molars (teeth 17 and 27): 11/21F1, 15/25F1 and 17/27F1. The mean passive centric line was calculated on two different segments: between central incisors and second

Table 3 Definition of relevant 3D measurements used in the analysis.

Measurement	Abbreviation	Definition
Angular measurements		
Temporal frontal inclination	∠STT-MRP	Mean angle between left and right Po-T lines and the vertical reference plane (VRP)
Temporal sagittal inclination	∠PoT-VRP	Mean angle between left and right ST-T lines and the median reference plane (MRP)
Skull width	T-T	Distance between left (Tl) and right (Tr) T-point landmarks
Cranial base angle	CBA	Angle between landmarks Na, S and Ba
SNA angle	∠SNA	Angle between landmarks S, N and A
SNB angle	∠SNB	Angle between landmarks S, N and B
ANB angle	∠ANB	Angle between landmarks A, N and B
Palatal plane inclination	∠PP-VRP	Angle between palatal plane (PP) and the vertical reference plane (VRP)
Anterior passive centric line of occlusion	PC1-5	Angle between the anterior passive centric line of occlusion (line between landmarks 11/21F1 and 15/25F1) and the FH plane
Posterior passive centric line of occlusion	PC5-7	Angle between the posterior passive centric line of occlusion (line between landmarks 15/25F1 and 17/27F1) and the Frankfort horizontal plane (FH)
Linear measurements		
Anterior cranial base length	S-N.length	Linear distance between landmarks S and N
Posterior cranial base length	Ba-S.length	Linear distance between landmarks Ba and S
Posterior cranial base depth	Ba-S.depth	Distance between landmarks Ba and S along the *x*-axis of the reference frame
Cranial base length	Ba-N.length	Linear distance between landmarks Ba and N
Cranial base depth	Ba-N.depth	Distance between landmarks Ba and N along the *x*-axis of the reference frame
Anterior midfacial height	AMH	Distance between landmarks N and ANS along the *y*-axis of the reference frame
Posterior midfacial height	PMH	Distance between landmarks S and PNS along the *y*-axis of the reference frame
Maxillary length	ANS-PNS.length	Linear distance between landmarks ANS and PNS
Dental arch width between 2nd premolars	5-5.width	Distance between landmarks 15F1 and 25F1 along the *z*-axis of the reference frame
Dental arch width between 2nd molars	7-7.width	Distance between landmarks 17F1 and 27F1 along the *z*-axis of the reference frame
Dento-alveolar height in the first incisor region	11/21-PP	Distance between landmarks 11/21F1 and plane PP along the *y*-axis of the reference frame
Dento-alveolar height in the 2nd premolar region	15/25-PP	Distance between landmarks 15/25F1 and plane PP along the *y*-axis of the reference frame
Dento-alveolar height in the 2nd molar region	17/27-PP	Distance between landmarks 17/27F1 and plane PP along the *y*-axis of the reference frame

premolars (anterior passive centric line of occlusion); and between second premolars and second molars (posterior passive centric line of occlusion), representing a more functional upper anterior and upper posterior occlusal plane, respectively (Fig. 2).

To better understand the impact of temporal bone sagittal (anterior/posterior) inclination on craniofacial morphology, the sample was subdivided into two subgroups based on the median value of the temporal bone sagittal inclination. Specimens with a mean temporal sagittal inclination > 57.25 ° were classified as the anterior rotation group (n = 82), and all others as the posterior rotation group (n = 81).

Statistical analysis was performed using Statistical Package for the Social Sciences software program Version 16.0 (SPSS, Chicago, USA). To determine intraobserver reliability and assess craniometric method error, 3D virtual models were again reconstructed from 16 skulls randomly selected, and all measurements were repeated by the same investigator after 3 weeks. Random and standard errors were calculated by correlation, which showed values between 0.76 and 0.99, and paired samples t-test between the first and second recordings. No systematic errors were detected ($P > 0.254$). Descriptive statistics including the means, standard deviations, minimums and maximums for all variables were calculated. All statistical tests were performed at the significance level of 1% ($\alpha = 0.01$). Correlation analysis was performed using Pearson product moment correlation coefficient. Differences between subgroups were evaluated using one-way ANOVA or Welch ANOVA (robust test of equality means), when theoretical assumptions were not verified.

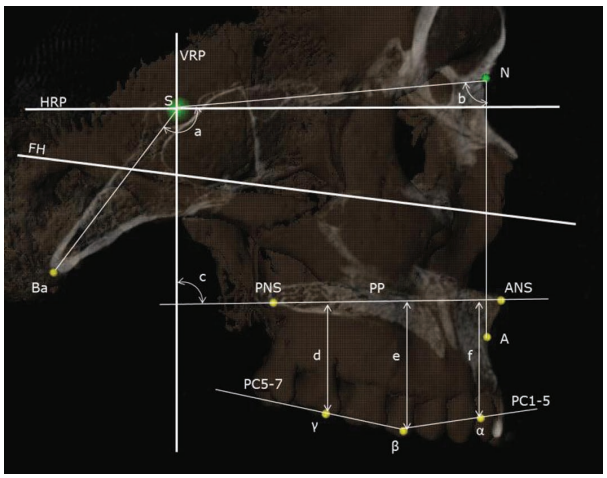

Fig. 2 Lateral view of a virtual skull (50% transparency) with the presence of the median sagittal tomographic volume slice. S, sella; N, nasion; Ba, basion; A, A-point; ANS, anterior nasal spine; PNS, posterior nasal spine; α, 11/21F1; β, 15/25F1; γ, 17/27F1; VRP, vertical reference plane; HRP, horizontal reference plane; FH, Frankfort horizontal plane; PP, palatal plane; PC1-5, anterior passive centric line of occlusion (between landmarks 11/21F1 and 15/25F1; inclination of this line was calculated relative to FH plane); PC5-7, posterior passive centric line of occlusion (between landmarks 15/25F1 and 17/27F1; inclination of this line was calculated relative to FH plane); a, cranial base angle (CBA); b, SNA angle; c, palatal plane inclination (∠PP-VRP); d–f, maxillary dento-alveolar height (17/27-PP, 15/25-PP and 11/21-PP, respectively; Specimen 09032).

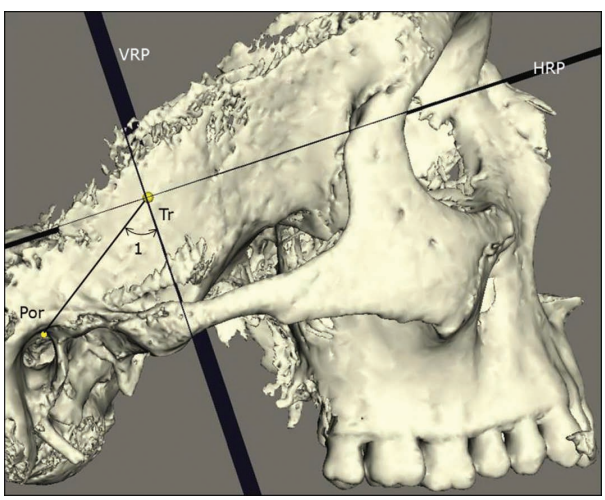

Fig. 3 Definition of temporal bone sagittal inclination. VRP, vertical reference plane; HRP, horizontal reference plane; Tr, right temporal point; Por, right porion; 1, temporal anterior/posterior inclination angle (∠PoT-VRP; Specimen 09008).

Results

Correlation coefficients between temporal bone variables and other craniofacial variables are shown in Table 4. The results show a positive correlation ($P < -0.01$) between the

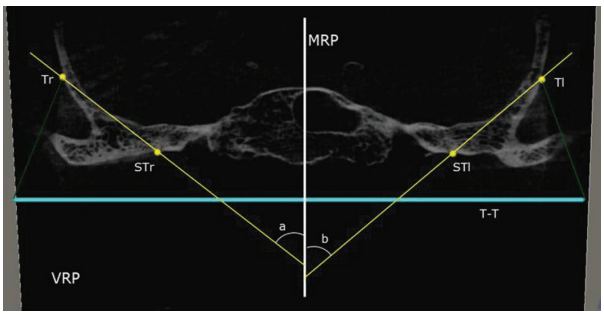

Fig. 4 View of the coronal CT slice of the tomographic volume at the same level as the vertical reference plane (VRP) representing the 3D measurement of frontal temporal bone inclination and skull width. MRP, median reference plane; Tr and Tl, right and left temporal points; STr and STl, right and left spheno-temporal points; a and b, right and left temporal bone frontal (medial/lateral) inclination angles (∠STT-MRP); T-T, skull width between left and right T-point landmarks (Specimen 09032).

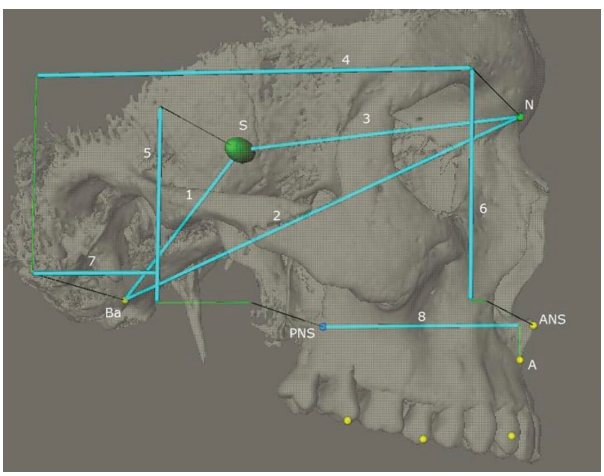

Fig. 5 Definition of linear measurements. S, sella point; N, nasion; Ba, basion; A, A-point; ANS, anterior nasal spine; PNS, posterior nasal spine; 1, posterior cranial base length (Ba-S.length); 2, cranial base length (Ba-N.length); 3, anterior cranial base length (S-N.length); 4, cranial base depth (Ba-N.depth); 5, posterior midfacial height (PMH); 6, anterior midfacial height (AMH); 7, posterior cranial base depth (Ba-S.depth); 8, maxillary length (ANS-PNS.length; Specimen 09032).

mean temporal sagittal inclination (∠Po.T-VRP) and the cranial base angle (∠Ba-S-N), the posterior cranial base depth (Ba-S.depth), the cranial base length and depth (Ba-N.length, Ba-N.depth), all of which represent different measurements of the antero-posterior dimension of the cranial base. Negative correlations ($P < 0.01$) were found between ∠Po.T-VRP and skull.width.T-T, ∠S-N-A, ∠S-N-B and the posterior midfacial height. These findings demonstrate that the more forward inclined the temporal bone is, the less flexed, antero-posteriorly longer and transversally narrower the cranial base is, the more retruded the anterior border of the maxilla and mandible are, and the shorter the posterior midfacial height also is. Interestingly, there is

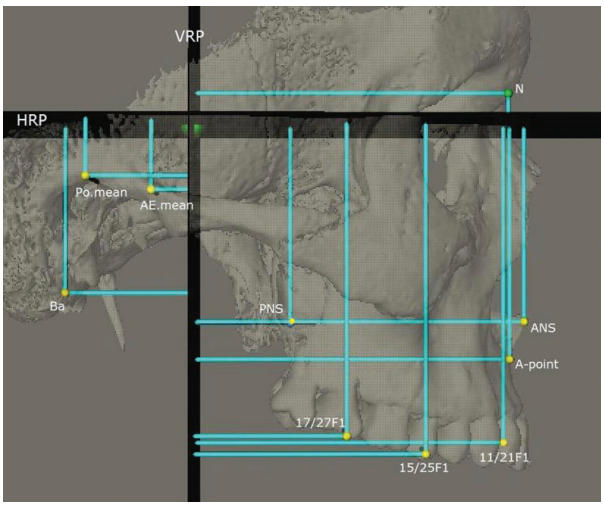

Fig. 6 Lateral view of a 3D surface model (50% transparency) representing orthogonal measurements of midline landmarks to the vertical reference plane (VRP) and horizontal reference plane (HRP). N, nasion; ANS, anterior nasal spine; A, A-point; Ba, basion; Po.mean, porion; AE.mean, articular eminence; PNS, posterior nasal spine; 11/21F1, mean center incisor functional point F1; 15/25F1, mean second premolar functional point F1; 17/27F1, mean second molar functional point F1 (Specimen 09032).

no significant correlation between temporal bone sagittal and frontal inclinations.

The mean frontal temporal inclination (∠ST.T-MRP) showed negative correlation ($P < 0.01$) with Ba-S.length, Ba-N.length and posterior midfacial height. A positive correlation ($P < 0.01$) was found with skull.width.T-T. These results suggest that greater internal inclinations of the temporal bone induce an antero-posteriorly longer skull base, a transversally wider skull and a higher posterior midfacial height.

The skull width between left and right T landmarks (skull.width.T-T) revealed negative correlations ($P < 0.01$) with ∠Ba-S-N and Ba-S.depth. No significant correlations were observed between temporal bone measurements and the upper dental arch width (5-5.width, 7-7.width), upper dento-alveolar height (11/21-PP, 15/25-PP and 17/27-PP), maxillary antero-posterior length (ANS-PNS.length) or jaw sagittal relationship (∠ANB).

The means and standard deviations for the posterior and anterior temporal rotation subgroup samples are shown in Table 5. Significant differences ($P < 0.01$) were found between both groups in cranial base angle (∠Ba-S-N), basicranium midline antero-posterior dimensions (Ba-S.depth, Ba-N.depth, Ba-N.length), skull width (T-T), mean porion vertical and horizontal position (Po.mean.coord-*x*, Po.mean.coord-*y*), mean articular eminence vertical and horizontal position (AE.mean.coord-*x*, AE.mean.coord-*y*), posterior midfacial height, palatal plane inclination (∠PP-VRP), maxilla position (∠SNA, A-point.coord-*x*, ANS.coord-*x*, PNS.coord-*x*), mandible position (∠SNB), posterior maxillary dentition position (15/25F1.mean.coord-*x*, 15/25F1.mean.coord-*y*, 17/27F1.mean.coord-*x*, 17/27F1.mean.coord-*y*), and in the inclination of the posterior passive centric line of occlusion (PC5-7). These findings reveal that in comparison with the posterior rotation group, the anterior rotation group has a less flexed and antero-posterior longer cranial base, a narrower skull, porion and the articular eminence are located more superiorly and posteriorly, the posterior midfacial height is shorter, the palatal plane is rotated clockwise, the maxilla and mandible are both more retrognathic, and the upper posterior occlusal plane is more inclined and posteriorly located. Figure 7 shows a schematic representation of the morphological characteristics in the posterior rotation and anterior rotation groups based on the average orthogonal position of midline anatomical landmarks relative to S point (zero point of the orthogonal reference system).

Table 4 Correlation coefficients between temporal bone variables and other craniofacial variables.

	Temporal frontal inclination	Temporal sagittal inclination	Skull width (T-T)
Temporal frontal inclination (∠STT-MRP)	–	005	219**
Temporal sagittal inclination (∠PoT-VRP)	005	–	−338**
Skull width (T-T)	219**	−338**	–
CBA (∠Ba-S-N)	−004	650**	−244**
S-N.length	−031	−038	133
Ba-S.length	−345**	−022	−032
Ba-S.depth	−175*	608**	−229**
Ba-N.length	−216**	238**	005
Ba-N.depth	−144	398**	−028
∠SNA	−040	−303**	031
∠SNB	−026	−369**	069
∠ANB	−022	074	−053
ANS-PNS.length	−017	102	030
Anterior midfacial height	−182*	064	048
Posterior midfacial height	−227**	−244**	108
5-5.width	−113	024	190
7-7.width	−036	−131	314
11/21-PP	−080	−060	141
15/25-PP	−053	−129	−059
17/27-PP	−098	−087	−034
PC1-5	007	−049	−132
PC5-7	040	−126	095

**$P < 001$; *$P < 005$.

Discussion

The results presented here provide significant support for the hypothesis of morphological integration between temporal bone sagittal (anterior/posterior) and frontal (medial/lateral) inclinations and facial morphology.

Table 5 Comparison of posterior (∠PoT-VRP ≤ 5725°) and anterior (∠PoT-VRP > 5725°) rotation groups.

	Posterior rotation group (n = 81)		Anterior rotation group (n = 82)		
	Mean	SD	Mean	SD	P
Temporal frontal inclination	4425	381	4458	540	
Temporal sagittal inclination	5222	396	6251	433	**
Skull width (T-T)	12 165	735	11 853	575	**
CBA (∠Ba-S-N)	13 058	450	13 580	448	**
S-N.length	6641	318	6601	302	
Ba-S.depth	2495	277	2816	290	**
Ba-S.length	4421	292	4416	271	
Ba-N.length	10 084	434	10 235	428	*
Ba-N.depth	9100	448	9381	447	**
∠SNA	8437	367	8244	384	**
∠SNB	8140	336	7919	376	**
∠ANB	297	282	325	252	
ANS-PNS.length	4512	246	4549	310	
Anterior midfacial height	5151	298	5184	351	
Posterior midfacial height	4409	259	4288	284	**
∠PP-VRP	9063	349	9248	315	**
PC1-5	−801	402	−839	414	
PC5-7	587	378	788	427	**
AE.mean.coord-x	−872	276	−1101	271	**
AE.mean.coord-y	−1882	247	−1600	232	**
Po.mean.coord-x	−2311	281	−2567	302	**
Po.mean.coord-y	−1796	242	−1363	252	**
A-point.coord-x	6631	400	6401	525	**
A-point.coord-y	−4977	332	−5027	413	
ANS.coord-x	6965	398	6768	469	**
ANS.coord-y	−4458	292	−4494	348	
PNS.coord-x	2131	274	1887	347	**
PNS.coord-y	−4411	258	−4291	283	**
Ba.coord-x	−2498	280	−2819	288	**
Ba.coord-y	−3637	354	−3389	327	**
N.coord-x	6602	312	6563	304	
N.coord-y	694	032	689	034	
11/21F1.coord-x	6277	466	6086	652	
11/21F1.coord-y	−6823	388	−6726	495	
15/25F1.coord-x	4879	478	4574	548	**
15/25F1.coord-y	−6983	383	−6819	423	*
17/27F1.coord-x	3306	456	2994	520	**
17/27F1.coord-y	−6670	386	−6528	427	*

(–) Vector that shows anterior area or superior area to point S.
(+) Vector that shows posterior area or inferior area to point S.
**P < 001; *P < 005.

Landmark T was geometrically constructed due to limitations in the field of view of the CBCT, which did not include the upper part of the temporal squama. Variation in such a geometrically defined landmark is not necessarily independent relative to the midsagittal structures that are used to define it, although it could be. To address this, the positional behavior of landmark T was evaluated and compared with that of the true anatomical landmarks porion (Po) and articular eminence (AE). Correlation was significant, with both landmarks along the x-axis (P < 0.05), y-axis (P < 0.01) and z-axis (P < 0.01) giving support to the likelihood that positional variations in landmark T are not caused by variation in Sella or Nasion or any other midline structure, but are actual variations of the lateral structures.

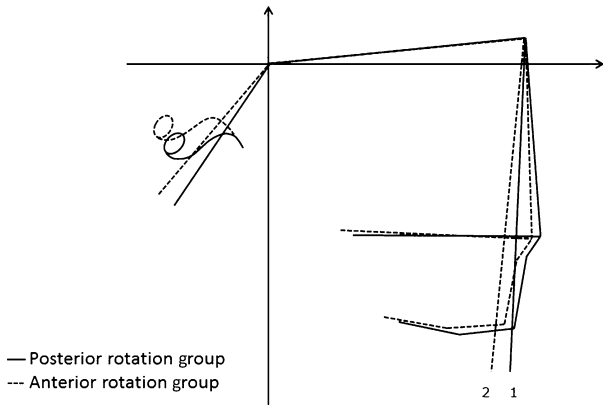

Fig. 7 Morphological characteristics in the anterior and posterior rotation groups. 1 and 2, nasion-B point line. See Fig. 6 for additional landmark identification.

The frontal inclination of the temporal bone (∠ST.T-MRP) shows a negative correlation (P < 0.01) with the total length of the cranial base (Ba-N.length) and the posterior cranial base (Ba-S.length), and a positive correlation (P < 0.01) with the skull width between T-point (T-T) landmarks, suggesting a behavior in which the increase in anterior–posterior length of the skull base (extension) leads to an internal rotation of the temporal bone, which in turn leads to a smaller transverse dimension of the skull. These results are in line with Sato's hypotheses towards the dynamic functional anatomy of the craniofacial complex (Sato, 2002).

The interaction between the width of the cranial base and the complex morphology of the face seems to be particularly important in humans, where the upper face is almost entirely located on the underside of the anterior cranial fossa. The most explicit of these hypotheses is that of Enlow (Enlow, 1990), which suggested that individuals with a rather narrow skull base tend to have a less flexed and antero-posteriorly longer cranial base, and a narrower face than individuals with a particularly wide skull base. He also proposed that individuals with a very narrow cranial base tend to have proportionately narrower and antero-posteriorly longer faces than individuals with a wider cranial base, which tend to have proportionately wider and antero-posteriorly shorter faces. This hypothesis has some support in studies on artificial deformation of human skulls. Anton (1989, 1994) shows that the antero-posterior compression of the head during the first years of life results not only in a wider neurocranium, but also in a concomitant wider face by further growth in the most lateral regions. Conversely,

the circumferential compression of the head results in narrowing of the neurocranium and face. Lieberman (2000) attempted to test Enlow's (1990) hypothesis on a sample of 98 adult skulls from five distinct populations. The results partially supported Enlow's hypothesis, showing that the width of the neuro-basicranial complex limits the width of the face, and that individuals with narrower skull base tend to have narrower and antero-posteriorly longer faces than individuals with wider skull bases. In the present study the transverse dimension of the skull between left and right T-point landmarks shows a negative correlation with cranial base flexion (∠Ba-S-N), posterior cranial base depth (Ba-S.depth) and temporal bone sagittal inclination (∠Po.T-VRP). These results are in line with Enlow's hypothesis (Enlow, 1990), but differ from the studies of Anderson & Popovich (1983), Solow (1966) and Björk (1955), who found no relationship between the cranial base width, flexion and length.

The findings of the present study show that the sagittal (anterior/posterior) inclination of the temporal bone is strongly related to the transversal width, flexion and antero-posterior length of the cranial base, to the anterior–posterior position of the mandible and maxilla, and to the posterior midfacial height. Surprisingly, the sagittal (anterior/posterior) inclination of the temporal bone has a greater impact on the 3D morphology of the craniofacial complex than that of its frontal (medial/lateral) inclination. We found no previous studies in the literature that have focused on the sagittal inclination of the temporal bone.

In order to better analyze the influence of temporal bone sagittal inclination (∠Po.T-VRP) on the craniofacial morphology, specimens were divided into two subgroups according to the median value of ∠Po.T-VRP. Significant differences were found between the anterior and posterior rotation groups. This hypothesis of morphological characteristics is shown in Fig. 6. In the anterior rotation group the cranial base was less flexed, antero-posteriorly longer and transversely narrower. Also, the posterior midfacial height was shorter, the palatal plane rotated clockwise, and the maxilla and mandible more retrognathic. The posterior passive centric line of occlusion (between 2nd premolars and 2nd molars) represents the upper posterior occlusal plane, which has been considered to be an important determinant of mandibular function and position (Fushima et al. 1996; Tanaka & Sato, 2008; Kim et al. 2009; Naretto et al. 2009). In this study, the anterior rotation group showed second premolars and second molars more distally and superiorly located, and a posterior passive centric line of occlusion (PC5-7) more inclined and posteriorly located. These results seem to support the hypothesis that a more inclined posterior occlusal plane is associated with a more retrognathic mandible, while a more horizontal posterior occlusal plane is associated with a more prognathic mandible.

It has been suggested that the spatial positioning of the mandibular fossa and its close relationship with the mandible could play an important role in the development of malocclusion. A more anterior position of the mandibular fossa has been associated with class III jaw relationship, and a more posterior position of the mandibular fossa with class II jaw relationship (Droel & Isaacson, 1972; Williams & Andersen, 1986; Baccetti et al. 1997; Basili et al. 2009; Innocenti et al. 2009). The vertical position of the mandibular fossa has also been suggested as a factor that might have important influence on face morphology. A more superior position has been associated with class II (high angle) jaw relationship, while a lower position was characteristic for class III (low angle) jaw relationship (Droel & Isaacson, 1972; Baccetti et al. 1997). In this study, the position of the mandibular fossa (landmark AE) was significantly different between the two subgroups, both in the *x*-axis and *y*-axis. The posterior rotation group revealed a more inferiorly and anteriorly located mandibular fossa (landmark AE), which was associated with a more anterior positioning of the mandible (B-point). However, no significant differences were found in skeletal jaw relationship (∠ANB), with A-point and B-point showing proportional differences in both subgroups. Porion (landmark Po) demonstrated a similar behavior to the mandibular fossa (landmark AE), possibly because of the anatomical proximity between these landmarks.

Concluding remarks

The findings of the present study suggest that differences in facial morphology are highly influenced by the spatial positioning of the temporal bones. Sagittal (anterior/posterior) inclination of the temporal bone seems to have a greater impact on the 3D morphology of the craniofacial complex than that of the frontal (medial/lateral) inclination of the temporal bone. However, more research is necessary to test in greater detail the hypothesis of morphological integration between temporal bone spatial positioning and facial morphology. This is a very complex interrelationship, and in evaluating skeletal disorders it is not just the anterior or posterior (sagittal) inclination of the temporal bone that may influence the craniofacial complex. Frontal inclination and torsion movement of the temporal bones also have to be considered, keeping in mind that all these movements may take place simultaneously and not necessarily with symmetry between the left and right side. Also, factors like the morphology and size of the mandible need to be considered as they also influence the development of the craniofacial complex and overall facial morphology.

Acknowledgements

This work was performed in the Research Institute of Occlusion Medicine and the Research Center of Brain and Oral Science, Kanagawa Dental College, and supported by a grant-in-aid for Open Research from the Japanese Ministry of Education,

Culture, Sports, Science and Technology. The authors would like to express their gratitude to the Ludwig-Slavicek Foundation, to Professor Maria Teschler-Nicola (Department of Anthropology, Museum of Natural History of Vienna) and to the research project postgraduate students (Skull Project) involved in the data collection process, especially Drs Tanaka EM, Fujii M, Taguchi C, Koizumi S, Sugimoto K, Sato C, Kodama T, Shinomiya M, Okada S, Horisawa A, Yamashita R, Takahashi T, Kim Y, Shirazu M, Park H, Kawai Y, Onodera K, Onodera Y and Tajima K.

References

Anderson D, Popovich F (1983) Relation of cranial base flexure to cranial form and mandibular position. *Am J Phys Anthropol* **61**, 181–187.

Anton S (1989) Intentional cranial vault deformation and induced changes of the cranial base and face. *Am J Phys Anthropol* **79**, 253–267.

Anton S (1994) Mechanical and other perspectives on neanderthal craniofacial morphology. In: *Integrative Paths to the Past: Paleoanthropological Advances in Honor of F. Clark Howell*. (eds Corruccini RS, Ciochon RL), pp. 677–695. Englewood Cliffs: Prentice Hall.

Baccetti T, Antonini A, Franchi L, et al. (1997) Glenoid fossa position in different facial types: a cephalometric study. *Br J Orthod* **24**, 55–59.

Bacon W, Eiller V, Hildwein M, et al. (1992) The cranial base in subjects with dental and skeletal Class II. *Eur J Orthod* **14**, 224–228.

Basili C, Costa H, Sasaguri K, et al. (2009) Comparison of the position of the mandibular fossa using 3D CBCT in different skeletal frames in human caucasic skulls. *J Stomat Occ Med* **2**, 179–190.

Bastir M, Rosas A (2005) Hierarchical nature of morphological integration and modularity in the human posterior face. *Am J Phys Anthropol* **128**, 26–34.

Bastir M, Rosas A (2006) Correlated variation between the lateral basicranium and the face: a geometric morphometric study in different human groups. *Arch Oral Biol* **51**, 814–824.

Bastir M, Rosas A, Kuroe K (2004) Petrosal orientation and mandibular ramus breadth: evidence for an integrated petroso-mandibular developmental unit. *Am J Phys Anthropol* **123**, 340–350.

Bastir M, Rosas A, O'Higgins P (2006) Craniofacial levels and the morphological maturation of the human skull. *J Anat* **209**, 637–654.

Bastir M, Rosas A, Lieberman DE, et al. (2008) Middle cranial fossa anatomy and the origin of modern humans. *Anat Rec (Hoboken)* **291**, 130–140.

Björk A (1955) Cranial base development: a follow-up x-ray study of the individual variation in growth occurring between the ages of 12 and 20 years and its relation to brain case and face development. *Am J Orthod* **41**, 198–225.

Brown AA, Scarfe WC, Scheetz JP, et al. (2009) Linear accuracy of cone beam CT derived 3D images. *Angle Orthod* **79**, 150–157.

Buschang PH, Baume RM, Nass GG (1983) A craniofacial growth maturity gradient for males and females between 4 and 16 years of age. *Am J Phys Anthropol* **61**, 373–381.

Celar A, Sato S, Akimoto A, et al. (1994) Sequential guidance with canine dominance in Japanese and Caucasian samples. *Bull Kanagawa Dent Coll* **22**, 18–24.

Costa H, Slavicek R, Sato S (2011) A three-dimensional computerized tomography study into the morphological interrelationship between anterior and posterior guidance and the occlusal scheme in human Caucasian skulls. *J Stomat Occ Med* **4**, 10–19.

Droel R, Isaacson R (1972) Some relationships between the glenoid fossa position and various skeletal discrepancies. *Am J Orthod* **61**, 64–78.

Ellis E, McNamara JA Jr (1984) Components of adult class III malocclusion. *J Oral Maxillofac Surg* **42**, 295–305.

Enlow DH (1990) *Facial Growth*. Philadelphia: W.B. Saunders.

Enlow DH, Bhatt M (1984) Facial morphology associated with headform variations. *J Charles H. Tweed Int Found* **12**, 21–23.

Enlow DH, Hans MG (1996) *Essentials of Facial Growth*. Philadelphia: W.B. Saunders.

Enlow DH, McNamara JA (1973) The neurocranial basis for facial form and pattern. *Angle Orthod* **43**, 256–270.

Enlow DH, Pfister C, Richardson E, et al. (1982) An analysis of black and caucasian craniofacial patterns. *Angle Orthod* **52**, 279–287.

Fushima K, Kitamura Y, Mita H, et al. (1996) Significance of the cant of the posterior occlusal plane in class II division 1 malocclusions. *Eur J Orthod* **18**, 27–40.

Harvati K (2003) Quantitative analysis of Neanderthal temporal bone morphology using three-dimensional geometric morphometrics. *Am J Phys Anthropol* **120**, 323–338.

Innocenti C, Giuntini V, Defraia E, et al. (2009) Glenoid fossa position in Class III malocclusion associated with mandibular protrusion. *Am J Orthod Dentofacial Orthop* **135**, 438–441.

Kerr WJ, Adams CP (1988) Cranial base and jaw relationship. *Am J Phys Anthropol* **77**, 213–220.

Kim JI, Akimoto S, Shinji H, et al. (2009) Importance of vertical dimension and cant of occlusal plane in craniofacial development. *J Stomat Occ Med* **2**, 114–121.

Lagravère MO, Carey J, Toogood RW, et al. (2008) Three-dimensional accuracy of measurements made with software on cone-beam computed tomography images. *Am J Orthod Dentofacial Orthop* **134**, 112–116.

Lavelle CLB (1979) A study of craniofacial form. *Angle Orthod* **49**, 65–72.

Lieberman D (2000) Ontogeny, homology, and phylogeny in the hominid craniofacial skeleton: the problem of the browridge. In: *Development, Growth and Evolution: Implications for the Study of Hominid Skeletal Evolution*. (eds O'Higgins P, Cohn M), pp. 85–112. London: Academic Press.

Lieberman DE, McCarthy RC (1999) The ontogeny of cranial base angulation in humans and chimpanzees and its implications for reconstructing pharyngeal dimensions. *J Hum Evol* **36**, 487–517.

Lieberman DE, Pearson OM, Mowbray KM (2000) Basicranial influence on overall cranial shape. *J Hum Evol* **38**, 291–315.

Lieberman DE, Hallgrímsson B, Liu W, et al. (2008) Spatial packing, cranial base angulation, and craniofacial shape variation in the mammalian skull: testing a new model using mice. *J Anat* **212**, 720–735.

Muramatsu A, Nawa H, Kimura M, et al. (2008) Reproducibility of maxillofacial anatomic landmarks on 3-dimensional computed tomographic images determined with the 95% confidence ellipse method. *Angle Orthod* **78**, 396–402.

Naretto S, Polastri C, Slavicek R (2009) Occlusal plane related to skeletal pattern in mixed dentition stage: a descriptive cephalometric study. *Int J Stomat Occ Med* **2**, 32–35.

Periago DR, Scarfe WC, Moshiri M, et al. (2008) Linear accuracy and reliability of cone beam ct derived 3-dimensional images constructed using an orthodontic volumetric rendering program. *Angle Orthod* **78**, 387–395.

Ross C, Henneberg M (1995) Basicranial flexion, relative brain size, and facial kyphosis in Homo sapiens and some fossil hominids. *Am J Phys Anthropol* **98**, 575–593.

Ross C, Ravosa M (1993) Basicranial flexion, relative brain size, and facial kyphosis in nonhuman primates. *Am J Phys Anthropol* **91**, 305–324.

Ross CF, Henneberg M, Ravosa MJ, et al. (2004) Curvilinear, geometric and phylogenetic modeling of basicranial flexion: is it adaptive, is it constrained? *J Hum Evol* **46**, 185–213.

Sato S (2002) The dynamic functional anatomy of craniofacial complex and its relation to the articulation of the dentitions. In: *The Masticatory Organ: Functions and Dysfunctions*. (ed. Slavicek R), pp. 482–515. Klosterneuburg: GAMMA Medizinisch-wissenschafttliche Fortbildungs-AG.

Scott JH (1958) The cranial base. *Am J Phys Anthropol* **16**, 319–348.

Singh GD, McNamara JA Jr, Lozanoff S (1997) Morphometry of the cranial base in subjects with Class III malocclusion. *J Dent Res* **76**, 694–703.

Slavicek R (1984) Die funktionellen Determinanten des Kauorganes. In: *Universitatsklinik fur Zahn-, Mund- und Kieferheilkunde* (ed. Schmitt WM), pp. 7–144. Wein: Verlag zahnärztlich-medizinisches Schrifttum.

Smith HF, Terhune CE, Lockwood CA (2007) Genetic, geographic, and environmental correlates of human temporal bone variation. *Am J Phys Anthropol* **134**, 312–322.

Solow B (1966) The pattern of craniofacial associations: a morphological and methodological correlation and factor analysis study on young male adults. *Acta Odontol Scand* **24**, 1–174.

Spoor F (1997) Basicranial architecture and relative brain size of Sts 5 (Australopithecus africanus) and other Plio-Pleistocene hominids. *S Afr J Sci* **93**, 182–186.

Swennen GR, Schutyser F, Barth EL, et al. (2006) A new method of 3-D cephalometry. Part I: the anatomic Cartesian 3-D reference system. *J Craniofac Surg* **17**, 314–325.

Tanaka EM, Sato S (2008) Longitudinal alteration of the occlusal plane and development of different dentoskeletal frames during growth. *Am J Orthod Dentofacial Orthop* **134**, 602 e1–602 e11; discussion 602–603.

Vannier MW, Marsh JL, Warren JO (1984) Three dimensional CT reconstruction images for craniofacial surgical planning and evaluation. *Radiology* **150**, 179–184.

Weidenreich F (1941) The brain and its role in the phylogenetic transformation of the human skull. *Trans Am Phil Soc* **31**, 320–442.

Williams S, Andersen CE (1986) The morphology of the potential Class III skeletal pattern in the growing child. *Am J Orthod* **89**, 302–311.

Young M (1916) A contribution to the study of the Scottish skull. *Trans R Soc Edinb* **51**, 347–343.